In-Vehicle Respiratory Rate Estimation Using Accelerometers

Ju WANG[1], Joana M. WARNECKE, Thomas M. DESERNO

Peter L. Reichertz Institute for Medical Informatics of TU Braunschweig and Hannover Medical School, Braunschweig, Germany

Abstract. The monitoring of vital signs in a dynamic environment is challenging. This work demonstrates an approach to estimate the respiratory rate (RR) under real-driving conditions by using two accelerometers for signal recording and de-noising. One accelerometer was attached to the seatbelt for recording respiratory movements; another one was attached to the left side of the car seat for recording noise. The frequency components of the noise were used to suppress the noise hidden in the signal. The performance of the proposed approach is evaluated for three testers under three driving conditions, i.e., *engine on*, *flat road* and *uneven road*. The estimated RRs for three testers are 11.54 ± 2.28 breaths per minute (bpm), 15.57 ± 5.77 bpm, and 9.63 ± 4.58 bpm. The median estimated RR for three testers are 12.08 bpm, 18.26 bpm, and 7.76 bpm, where the manually counted reference RRs are 12 bpm, 18 bpm, and 7 bpm respectively. The average difference between estimated RRs and reference RRs is 0.71 bpm for the condition *engine on*, 3.36 bpm for *flat road*, and 4.58 bpm for *uneven road*. The results exhibit the ability of the proposed approach to estimate RR under real-driving conditions.

Keywords. Respiration monitoring, respiratory rate, accelerometer, sensor, in-vehicle monitoring

1. Introduction

For many people, a car is an important living space, where people spend a considerable amount of time. As the way of driving is changing towards assisted or autonomous driving [1], an in-vehicle regular medical check-up may be more feasible than ever [2, 3]. Therefore, a vehicle can be turned into a diagnostic space. To this end, the issue of monitoring vital signs in a dynamic environment such as in a moving car should be addressed. A meaningful vital sign is respiration, which can indicate a variety of pathological conditions including respiratory, cardiovascular and metabolic disorders [4].

The use of health enabling technologies can advance the monitoring of respiratory-related parameters, such as respiratory rate (RR). Since respiration induces rhythmical body movements, microelectromechanical sensors (MEMS) mounted on a certain part of the body (e.g., chest wall) are usually applied to monitor respiration. For instance, by using accelerometers on the chest wall, the respiratory rate can be measured during different breathing conditions [4]. Respiratory flow waveforms can also be estimated from accelerometer data [5]. This low-cost and unobtrusive device can be used for

---

[1] Corresponding author, Peter L. Reichertz Institute for Medical Informatics of TU Braunschweig and Hannover Medical School, Braunschweig, Germany; E-mail: ju.wang@plri.de.

screening breath disorders such as obstructive sleep apnea, to support other clinical diagnostic approaches, e.g., gating technique in obtaining motion-free images [6, 7].

Nevertheless, the current research mainly investigates respiration monitoring under static environments. In-vehicle monitoring is still challenging due to the unstable environment such as the vibration from the moving vehicle, the running engine and the artifact from the human body [8, 9]. The objective of this work is to demonstrate an approach to estimate respiratory rate under real-driving conditions for autonomous driving using two accelerometers for signal recording and de-noising at the passenger seat.

2. Methods

2.1. Measurement System

We set up a measurement system in a test vehicle (Mini One, 66 kW, BMW, Munich, Germany) using two sensor modules with three-axis accelerometers (Shimmer3 IMU, Shimmer, Ireland), and a laptop (Latitude 5480, Dell, Texas, USA). The sensors can generate accelerometers accompanied with UNIX timestamps. Based on our previous experiment experience, the position of side-waist can best reflect the respiratory movements [10]. To monitor the respiratory movements, one sensor was attached to the seat belt at the position side-waist, namely Sensor I. To record noise from the environment, another sensor was attached to the left side of the passenger seat, i.e., Sensor II (Fig. 1). The sampling rates for both sensors were configured as 204.8 Hz. The laptop was carried in the vehicle for storing and observing the respiratory movement data in real-time. Sensor I was connected to the laptop via Bluetooth. Sensor II stored the data in its local SD card, and the data were manually transferred to the laptop after the experiment.
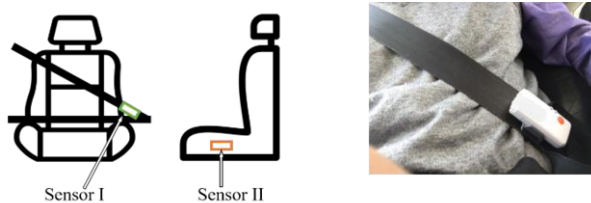
Figure 1. The positions of two sensors on the passenger seat.

2.2. Experiment

We designed an experiment covering three driving-conditions. As a preliminary work, three healthy volunteers participated in the experiment as testers. The BMI for male Tester 1 (T1) was 20.8, for female Tester 2 (T2) 22.0, and for male Tester 3 (T3) 23.4.

Each tester was required to sit in a state of relaxation on the passenger seat where the sensors were placed. The test vehicle was driven under three conditions: (1) *Engine on*: start the engine but keep the vehicle in a parking lot; (2) *Flat road*: drive the vehicle on a flat surface without potholes at a speed 20 - 30 km/h. (3) *Uneven road*: drive the vehicle on a gravel parking lot at a speed 10 ± 2 km/h. The duration for each driving condition was 2 - 3 minutes, i.e., a session. Each tester experienced four sessions under one condition. Therefore, we collected the datasets consisting a total of 36 sessions.

2.3. Data Processing

Sensor I generates data containing signal and noise, while the Sensor II generate data purely containing noise. A preprocessing pipeline was applied to the data of both sensors (Fig. 2).

(1) *Band-pass filter*: A Butterworth band-pass filter was applied to tri-axial acceleration a(x, y, z). Because the normal RR range is 8 to 20 breaths per minute (bpm) [11, 12], the cutoffs were configured as [0.05 Hz, 1 Hz], which were commonly used for extracting respiratory information [7, 13]. After this step, we obtained filtered acceleration a'(x, y, z).

(2) *Principal Component Analysis (PCA)*: The PCA was applied to the filtered acceleration, and the first principal component (PC) was selected as the fusion of the tri-axial data, which is p.

(3) *Fast Fourier transformation (FFT)*: The PC was transformed from the temporal domain to the frequency domain using FFT. We selected the series referring to the frequency interval [0.05 Hz, 1 Hz]. After this step we obtained the Fourier series P.
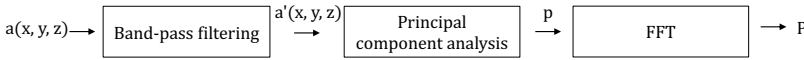
Figure 2. Data preprocessing pipeline.

After the preprocessing, we obtained two Fourier series P_1 and P_2 for each session. The magnitudes of P_1 represent the frequency distribution of the mixture of the vital signal and noise, whereas the magnitudes of P_2 represent the frequency distribution of the noise. Given a frequency component, the higher magnitude implies higher noise at the frequency component. Thus, we defined a suppressing factor (SF) aiming to suppress the frequency components in P_1, where the noise is higher in P_2. The kth SF can be calculated by the suppressing function,

$$SF[k] = e^{-\frac{|P_2[k]|}{\frac{1}{N}\sum_{i=1}^{N}|P_2[i]|}}$$

The frequency distribution of the noise-inhibited signal can be obtained by $SF \cdot P_1$. The highest peak in the targeting frequency interval [0.05 Hz, 1 Hz] can be used to derive the corresponding frequency RR_e. The whole process can be summarized as shown in Fig. 3.
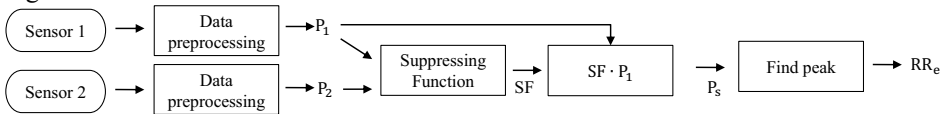
Figure 3. Data processing flowchart.

2.4. Results Evaluation

To evaluate the RR_e, we determined the reference RRs for all testers before the experiment. We observed testers' respiration when they were in a state of relaxation and calculated their average RRs. We assume that a healthy person's RR remains stable when

she/he has no active movements within a short term. The reference RRs are manually observed as 12 bpm, 18 bpm, 7 bpm for T1, T2, and T3 respectively. The differences between the estimated RRs and the reference RRs were compared across conditions and testers.

3. Results

3.1. Results of Data Processing
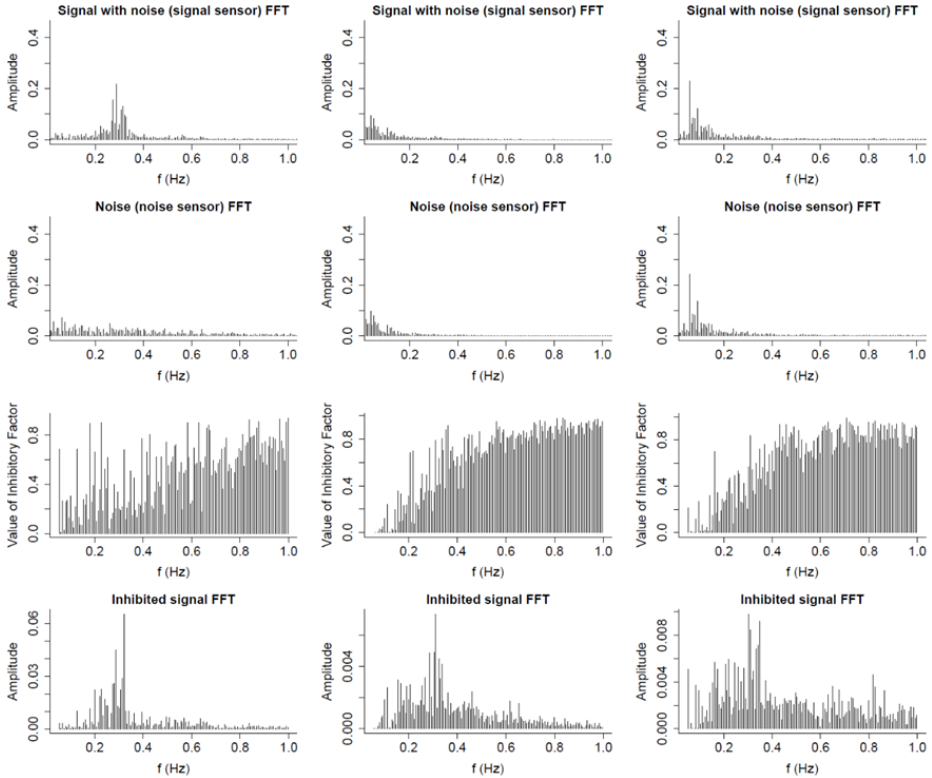
Figure 4. FFTs of Sensor I data and Sensor II data of three driving conditions: engine on (column 1), *flat road* (column 2) and *uneven road* (column 3).

The FFTs of Sensor I data reflect the frequency component distribution of a mixture of the vital signal and noise. The FFTs of Sensor II data reflect the frequency component distribution of the noise. The results confirm that both signal data and noise data have similar low-frequency distribution (Fig. 4). Applying the SF function to the noise FFT, we obtain a vector of SF. To apply the IF to the Sensor I data, some components of the low-frequency noise can be reduced and the signal is highlighted (Fig. 4 row 4).

3.2. Comparison of Estimated and Reference RRs

The estimated RRs for the three testers are 11.54 ± 2.28 bpm, 15.57 ± 5.77 bpm, and 9.63 ± 4.58 bpm. The estimated RRs are distributed around the testers' reference RRs

(Table I). The approach performs the best on T1's. The medians (Q2) of estimated RRs for all testers are close to their reference RRs (Fig. 5, left). From the perspective of the driving environment, we calculated the difference between the estimated RRs and the reference RRs. The results show that under the condition *engine on*, we have the best estimation, with an average difference of 0.71 bpm and the lowest variance of difference (Fig 5, right). Under the condition of *flat road*, the average difference is 3.36 bpm; and under the condition of *uneven road*, the average difference is 4.58 bpm.

Table 1. The median (Q2) and the 25% and 75% quantiles (Q1, Q3) of three testers' estimated RRs.

Tester	Q1 (bpm)	Q2 (bpm)	Q3 (bpm)	Reference RR (bpm)
T1	11.18	12.08	12.61	12
T2	14.62	18.26	19.11	18
T3	6.86	7.76	12.25	7
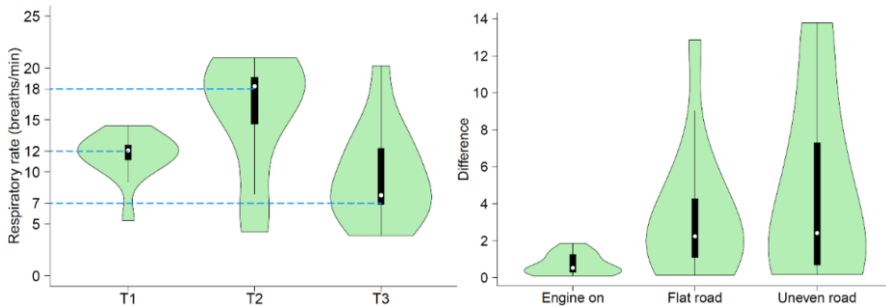
Figure 5. Violin plots of estimated RRs as for three testers (left) and the difference between estimated RRs and reference RRs for three driving conditions (right). The reference RRs are labeled by dashed blue horizontal lines (left).

4. Discussions and Future Work

With an additional sensor to intentionally record noise, the pure noise frequency components can be revealed. Based on the noise information, the suppressing factor is a more reasonable approach than directly subtraction in frequency domain between the two data sources. The results, including the distribution of estimated RRs and the average errors, exhibit the ability to de-noise respiratory signal in the frequency domain using an additional sensor.

The results show the variance for different testers. The reasons could be the difference in the body sizes between individuals like females and males. The body size could affect the movements of the seatbelt induced by respiration. The orientation of the signal sensor varies for large and small body sizes. The respiratory depth also varies between individuals, which can influence the amplitude of sensor data.

The results also demonstrate the difference of performance for the three selected driving conditions. Under the condition *engine on*, we can obviously get the most stable estimation in the given experiment. Even the variance of difference for *flat road* is larger than *uneven road*, it can still produce more centralized distribution than the *uneven road*. With *engine on*, the main noise comes from the high-frequency components and nearly no distortion on the signal. Unlike *engine on*, low-frequency components can be brought in when the car is driven on road. *Uneven road* means more low-frequency than *flat road*.

In this work, the simulated autonomous driving simplified the question of separating the signal from noise. More artifacts are possibly to be brought and many factors will affect the smoothness of breathing in regular traffic, such as congestion, aggressive drivers, mood of the driver. All these factors should be investigated in the future.

One limitation of the current work is the manually observing reference RRs. A piezo respiration sensor placed on the chest and abdomen can be used to obtain more precise reference RRs [14]. The placement of the additional sensor for noise recording might be optimized. So far it is still unknown whether the placement of the noise sensor can influence the performance of estimation and which position could be the best choice. As a preliminary research, only healthy testers are participated. Unhealthy or patient with respiratory disease like COPD patient should be included and the sample size should be scaled up in in future work.

The noise difficulty is unavoidable in estimating vital signs when implementing pervasive healthcare. The knowledge and experience acquired in this work might be generalizable to measurements of other vital signs using accelerometers such as the ballistocardiography (BCG).

References

[1] Mogelmose A, Trivedi MM, Moeslund TB. Vision-based traffic sign detection and analysis for intelligent driver assistance systems: perspectives and survey. IEEE Trans Intell Transp Sys. 2012;13(4):1484–97.
[2] Zheng R, Yamabe S, Nakano K, Suda Y. Biosignal analysis to assess mental stress in automatic driving of trucks: palmar perspiration and masseter electromyography. Sensors. 2015;15(3):5136–50.
[3] Baek HJ, Lee HB, Kim JS, Choi JM, Kim KK, Park KS. Nonintrusive biological signal monitoring in a car to evaluate a driver's stress and health state. Telemed J E Health. 2009;15(2):182–9.
[4] Lapi S, Lavorini F, Borgioli G, Calzolai M, Masotti L, Pistolesi M, Fontana GA. Respiratory rate assessments using a dual-accelerometer device. Respir Physiol Neurobiol. 2014;19160–6.
[5] Bates A, Ling MJ, Mann J, Arvind DK. Respiratory rate and flow waveform estimation from tri-axial accelerometer data. In: Ling KV, editors. BSN 2010: Proceedings of the 2010 International Conference on Body Sensor Networks; 2010 Jun 7-9; Singapore. Piscataway: IEEE; 2010. p. 144–50.
[6] Jafari Tadi M, Koivisto T, Pänkäälä M, Paasio A. Accelerometer-based method for extracting respiratory and cardiac gating information for dual gating during nuclear medicine imaging. Int J Biomed Imaging. 2014;2014690124.
[7] Dehkordi PK, Marzencki M, Tavakolian K, Kaminska M, Kaminska B. Validation of respiratory signal derived from suprasternal notch acceleration for sleep apnea detection. In: Lovell N, editors. EMBC 2011: Proceedings of the 2011 Annual International Conference of the IEEE Engineering in Medicine and Biology Society; 2011 Aug 30 - Sep 3; Boston, MA, USA. Piscataway: IEEE; 2011. p. 3824–7.
[8] Walter M, Eilebrecht B, Wartzek T, Leonhardt S. The smart car seat: personalized monitoring of vital signs in automotive applications. Personal and Ubiquitous Computing. 2011;15(7):707–15.
[9] Wusk G, Gabler H. Non-invasive detection of respiration and heart rate with a vehicle seat sensor. Sensors. 2018;18(5).
[10] Wang J, Warnecke JM, Deserno TM. The vehicle as a diagnostic space: efficient placement of accelerometers for respiration monitoring during driving. In: Shabo A, Madsen I, editors. EFMI STC2019: Proceedings of the EFMI Special Topic Conference; 2019 Apr 7-10; Hannover, Germany. Amsterdam: IOS; 2019. p. 206-10.
[11] MedlinePlus. Vital signs [Internet]. 2019 [updated 2019 Jan 7; cited 2019 Jan 20]. Available from: https://medlineplus.gov/ency/article/002341.htm
[12] MedlinePlus. Rapid shallow breathing [Internet]. 2019 [updated 2019 Jan 7; cited 2019 Jan 20]. Available from: https://medlineplus.gov/ency/article/007198.htm
[13] Jarchi D, Rodgers SJ, Tarassenko L, Clifton DA. Accelerometry-based estimation of respiratory rate for post-Intensive care patient monitoring. IEEE Sensors J. 2018;18(12):4981–9.
[14] Hamdani STA, Fernando A. The application of a piezo-resistive cardiorespiratory sensor system in an automobile safety belt. Sensors. 2015;15(4):7742–53.